

WORKING PAPER 348

"Models for soil evolution on slopes"

M.J. Kirkby
School of Geography
The University
Leeds LS2 9JT
England

London
George Allen & Unwin
Boston Sydney

February 1983

ABSTRACT

The paper explores the main ways in which parent material and soil influence hillslope form. Proposals are made for simple functional relationships for each linkage with some discussion of alternatives and their implications. The main processes discussed are solute pick-up, soil profile development, mechanical transport in thin soils, hillslope hydrology, creep, solifluction, wash and landsliding. Each process is discussed at a minimal level to obtain useable relationships in a general model. These components have been assembled into a small numerical model and illustrative simulations have been carried out. Qualitative comparisons with real slopes are encouraging, but no detailed validation has yet been carried out.

MODELS FOR SOIL EVOLUTION ON SLOPES

1. INTRODUCTION

The intention of this paper is to explore the relationships between rock type and slope form, mediated by the soil. It puts forward as simple an explanatory theory as is considered reasonable, and examines its assumptions and geomorphological implications through a series of related models. Knowledge of this relationship is a major gap in our understanding of how landforms evolve, and has received less attention than its importance warrants. Perhaps the most serious attempts have been those by Ahnert (1964) and Huggett (1975) but the former, although an important step, has insufficient basis, while the latter does not extend far enough towards landform development.

The assumptions underlying the present approach are that rock type has two, or perhaps three, major influences which are able to act through its regolith or soil cover. Rock type is thought to influence (a) rates of solutional denudation, (b) geotechnical properties of the soil and (c) rates of percolation to groundwater through the rock mass and its voids network. Climate is seen as a second, independent, control on slope hydrology, which in turn determines the partition between overland and subsurface flow on the hillside. The current slope morphology acting largely through slope gradients, influences rates of landslide, creep/solifluction and wash transport. With soil depth, it also has an influence on

slope hydrology, by setting an upper limit on sub-surface discharge. The combination of mechanical and solutational denudation control the evolution of both the slope profile and the soil on it. The interactions considered are summarized in Figure 1, and the selection of these links as predominant is a first crucial step in explanation. The second level is to examine some of the interactions shown in greater detail, and examine suitable functional forms for each within an overall model, as well as explaining why some possibly relevant linkages have been omitted. Before doing so however, the governing mass balance equations should be briefly stated in a consistent notation.

Mass balance for a section of a slope profile may be expressed in the form:

$$-\partial z / \partial t = -\partial / \partial x (S + V) \quad (1)$$

where z = elevation above an arbitrary datum measured in rock equivalent depths,

t = time elapsed,

x = horizontal distance from the divide,

S = mechanical sediment transport,

and V = solute transport.

Expressions of this general form have been widely used since the 1960's (e.g. Ahnert 1967, Culling 1963) at least. In this formulation it is assumed that the slope profile is of uniform width which is not changing over time, and that there is negligible direct aerial input or output of sediment.

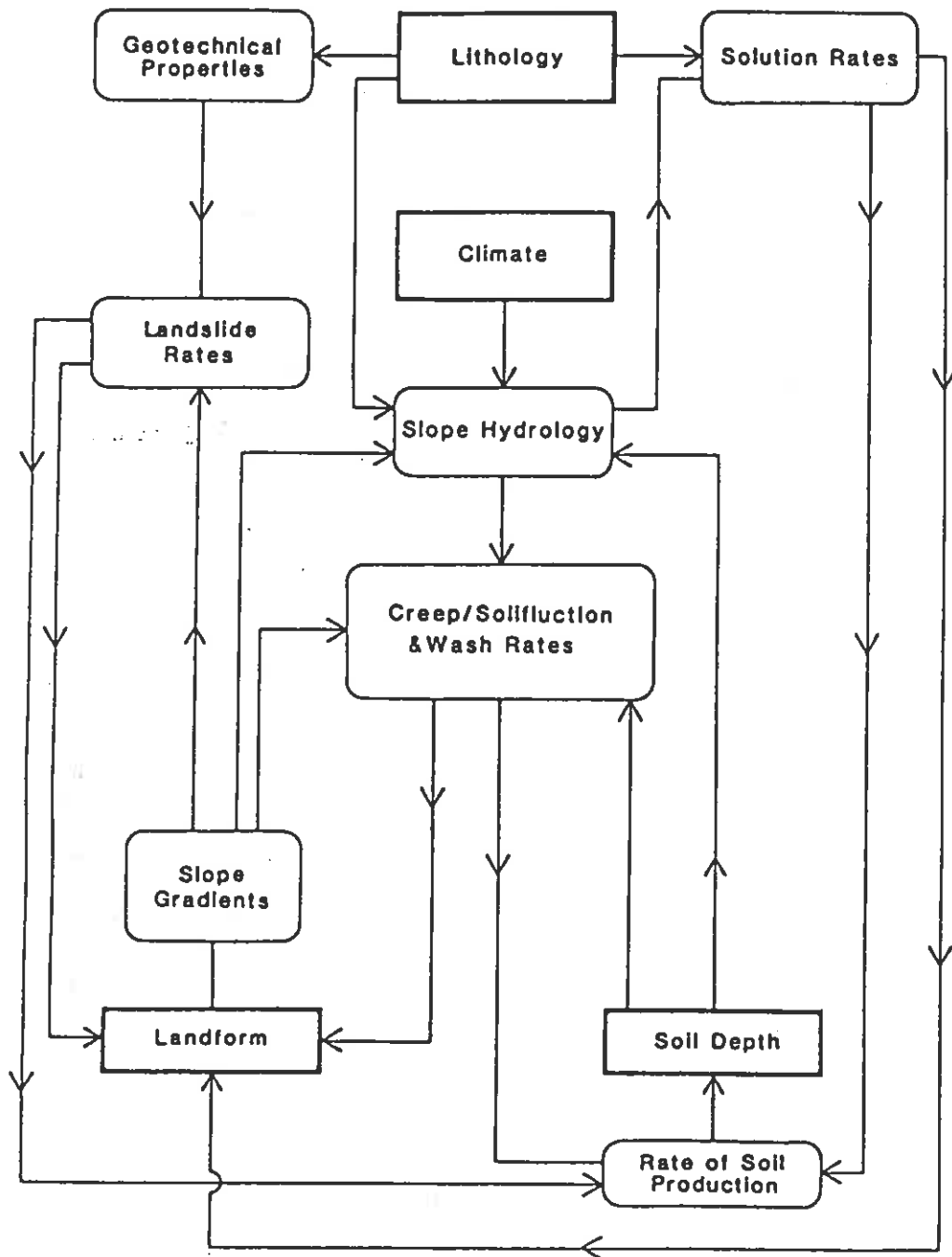


Figure 1. Linkages considered in the models discussed.

In a similar way, a mass balance may be defined for soil, using the concept of "soil deficit" (Kirkby 1976b). The degree of weathering at depth y within the soil may be described by the proportional substance remaining, p . Thus $p = 1$ for bedrock and decreases with weathering. The soil deficit is then defined as

$$w = \int_{y=0}^{\infty} (1-p) dy \quad (2)$$

This quantity has the dimension of depth and normally increased monotonically with it, but is more precisely defined where the weathering front is diffuse. The balance for soil deficit is then:

$$\partial w / \partial t = \partial / \partial x (V - S \pi_x) \quad (3)$$

where $\pi_x = (1-p_s)/p_s$ and p_s is the proportional substance near the surface (beneath the A horizon).

This equation expresses the balance between addition to the soil by weathering and loss by mechanical denudation, which takes place at the surface.

2. LITHOLOGY AND SOLUTE CONCENTRATION

The first linkage to be considered in detail is that between lithology and solution rate, assuming a known subsurface flow. The rate of solute pick-up (i.e. volumetric concentration) should tend asymptotically to a concentration characteristic of rock type downslope from a lithological boundary. In addition the total solute

load should be zero at the divide and should not change discontinuously at a lithological contact. It is argued that equilibrium thermodynamic models for solution are more relevant than kinetic models because residence times in the soil matrix are long enough (> 100 hours say) to approach equilibrium with the current soil solids. It is also argued, partly from exploration of soil profiles, that most solution occurs from the base of the soil, within a zone where soil and bedrock compositions differ little. Three alternative formulations were considered for the solute pick-up within a zone of constant lithology. They are:

- (a) $dV/dq = c$ (4)
- (b) $V = cq$
- (c) $dV/dq = (cq - V)/q_*$

where q is the subsurface flow discharge which is assumed to come into chemical equilibrium with the rock/soil;

c is a characteristic concentration for the rock;

and q_* is a characteristic discharge.

The first (a) assumes local rates of pick-up to depend on local lithology and that the overlying soil can maintain solute load from upslope. (b) assumes that the total load reaches instantaneous equilibrium with local lithology, thus giving discontinuities in load at a lithological boundary. (c) assumes that some load carrying capacity is lost as the soil from upslope is lost by mechanical erosion, and that a compensating load is picked up from bedrock to approach equilibrium: the constant q_* here represent the distance downslope for which soil survives before it is lost by erosion. Although in most ways the most conceptually attractive model, it

gives, for transport near the origin:

$$\underline{V} = Ux - Ux_0 \left[1 - \exp(-x/x_0) \right]$$

where $\underline{U} = c \left[dq/dx \right]_{x=0}$

This expression behaves like

$$\underline{V} \simeq Ux^2/(2x_0)$$

which would give no weathering at divides, in contradiction to observation. Model (c) is therefore rejected and (a), which seems to have least disadvantages, is adopted here.

3. SOIL DEFICITS AND SOIL WEATHERING

In order to solve the mass-balance equation for soil deficit, an additional relationship is required. Even when the geomorphic environment, as defined by the transport rates S and \underline{V} , is known, then π_g and w still represent independent soil variables. The simplest approach is to note that the course of soil weathering should produce consistent increases in both soil deficit and the ratio π_g . Explorations of a soil profile model (Kirkby 1976a, 1982) suggest that this relationship is substantially unique for a given parent material and climate, and is substantially unaffected by changes in the rate of mechanical denudation. Thus π_g may be expressed as a function of soil deficit, w . It appears further that for small deficits, the function is essentially linear, corresponding to an exponential decay curve of the form:

$$p = 1 - Ae^{-bw}$$

for constants A , b . This form is related to the dominance of ionic

diffusion for transferring solutes upwards from bedrock into the soil. It has also been shown that for large deficits, π_s tends to a constant upper value, π_k . This corresponds to the observed rather constant composition of lateritic and other deeply weathered profiles at $\pi_k = 1$ to 1.5. A simple and suitable functional form for the relationship is:

$$\pi_s = \pi_k w / (w + w_1) \quad (5)$$

for constants π_k , w_1 which describe respectively the limiting value and the slope of the linear relationship for small deficits.

Appropriate values for w_1 are thought to be about 1-2 m. The form of Equation 5 and the set of soil profiles associated with it is shown in Figure 2. The general course of soil development at a site may readily be seen from Equations 3 and 5, if it is assumed that denudation rates are constant over time, and that the variation in soil deficit downslope may be neglected. In that case Equation 3 reduces to:

$$\frac{dw}{dt} = U - T \frac{\pi_k w}{w + w_1} \quad (6)$$

where $U = dV/dx$ and $T = dS/dx$.

The relevant solution is then:

$$t = \frac{w}{U - T\pi_k} - \frac{T\pi_k w_1}{(U - T\pi_k)^2} \ln \left[\frac{w(U - T\pi_k)}{w_1 U} + 1 \right] \quad (7)$$

The soil tends towards an equilibrium if $T\pi_k > U$, at deficit:

$$w = \frac{U w_1}{T\pi_k - U}$$

and at $\pi_s = U/T$.

If however $T\pi_k \leq U$ then the soil thickens indefinitely.

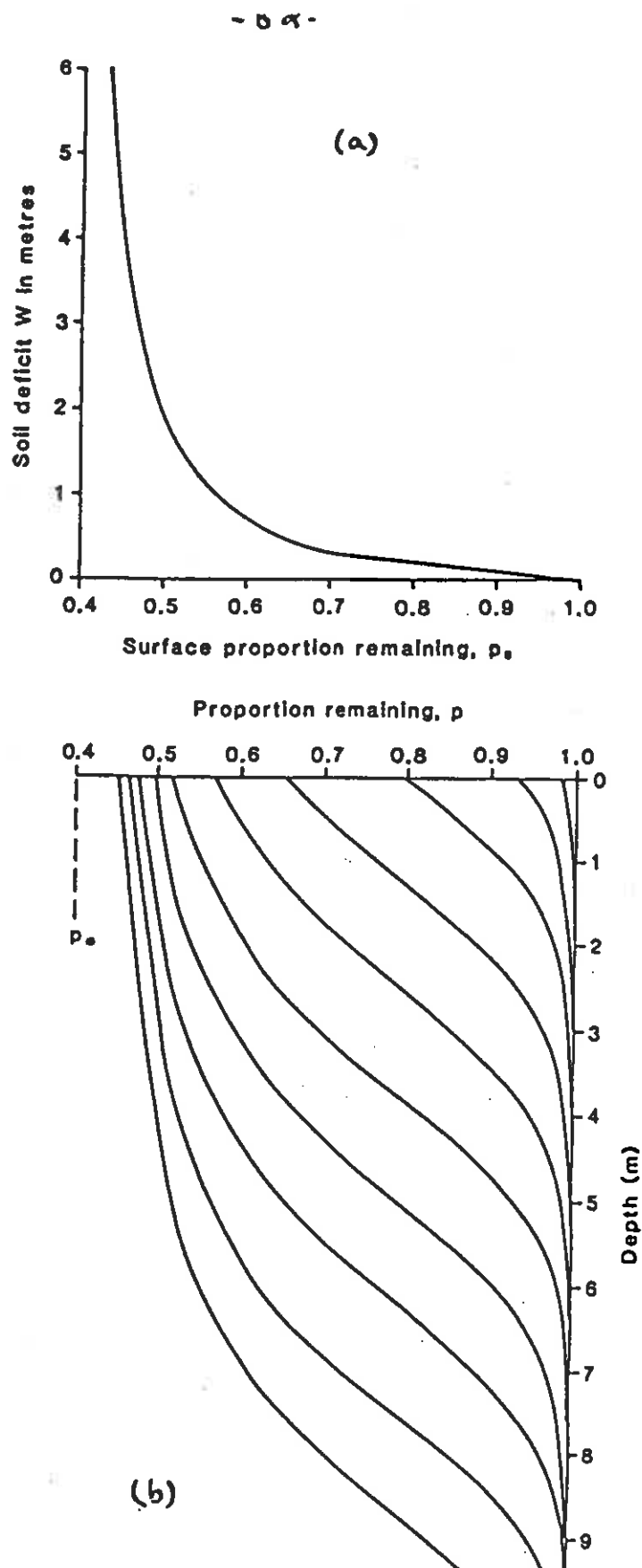


Figure 2. (a) The relationship between degree of surface weathering, p_s and total soil deficit, w given by Equation 5.
 (b) The implicit sequence of soil profile evolution (at approximately equal time intervals).

Curves drawn for $p_s = 0.4$; $\pi_s = 0.5$; $w = 1$ m

This expression is illustrated in dimensionless form in Figure 3. Reasonable values for chemical denudation range from 0.1 to 10 mm/year for igneous rocks and from 0.1 to 100 mm/year for limestones, in both cases increasing with climate. For values of the soil weathering constants

$$\pi_1 = 1 \quad \text{and} \quad \pi_2 = 1 \text{ m}$$

the constants in Figure 3 are as follows:

Igneous rocks		Limestones	
Arid	Humid	Arid	Humid
0.1	10	0.1	100
0.1	10	0.1	100
10^7	10^5	10^7	10^4

U = rate of solutional denudation
 T^1 = Minimum rate of mechanical denudation for equilibrium
 w_1/U = Scale Multiplier to connect time axis to years

Figure 3a shows the general course of soil deficit evolution. Taking a central value of $U = 5 \mu\text{m/yr}$, it may be seen that negligible divergence occurs until $Ut/w_1 = 0.25$; that is for the first 50 000 years, except under very rapid mechanical stripping. Post-glacial soil evolution is therefore not expected to show much sensitivity to site factors which control mechanical stripping except perhaps on the steepest slopes ($T > 50 \mu\text{m/year}$). Figure 3b shows the times taken to approach equilibrium, which are considerable, especially close to the critical value of T . Thus, for the example value of $U = 5 \mu\text{m/year}$, and a mechanical denudation of twice the critical value ($10 \mu\text{m/year}$), the soil takes 490 000 years to attain 80% of its equilibrium deficit. In this time, the total landscape denudation is $490\,000 \times [(5 + 10) \times 10^{-6}] \approx 7.5 \text{ m}$. Although

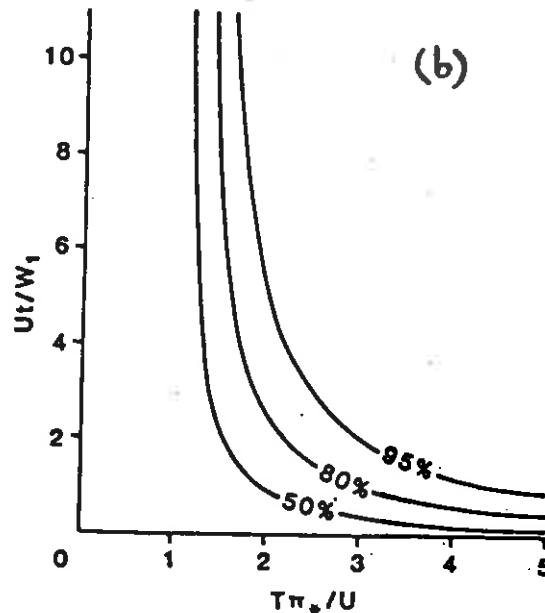
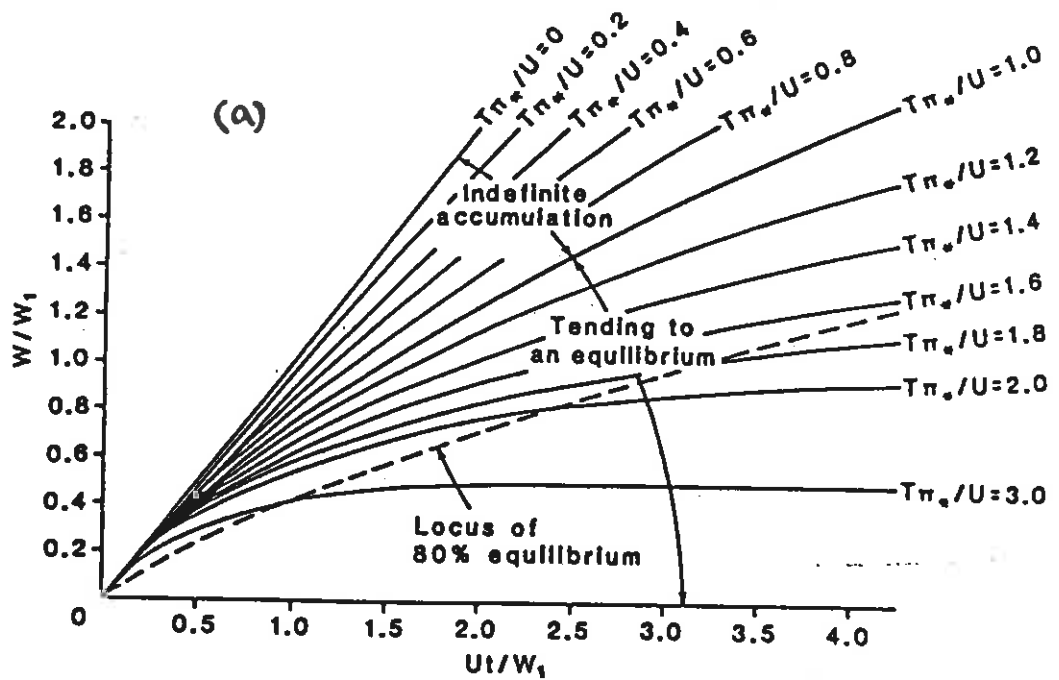


Figure 3. Model soil development over time under constant conditions of solute and mechanical denudation.

(a) Soil deficit as a function of time elapsed. Broken line shows locus of points for which soil deficit has reached 80% of its equilibrium value.

(b) Times taken to reach different percentages of equilibrium deficit, in terms of relative rates of mechanical and solutional denudation.

appreciable, this erosion loss normally represents a small fraction of the available relief (150 m on average for a denudation of $15 \mu\text{m}/\text{year}$ Ahnert (1970)). It is therefore argued that the assumption of constant denudation during soil development is sufficiently met, and that equilibrium soils should occur as a normal feature of "mature" landscapes. Indeed on landscapes eroding at very rapid rates of 1 mm or more annually, equilibrium soils (admittedly rather thin) will be approached (50% level) in a period of only 1000 years, when only 1 m of total stripping has occurred. This model forecasts a downslope soil catena associated with weathering. For example, if constant solutational loss, U is assumed downslope, then for a normal "mature" slope down which mechanical loss decreases downslope, a soil catena will be developed of deepening soils downslope. Equilibrium will be approached soonest near the divide, where denudation is most rapid, and progressively later, if at all, at successive sites downslope.

4. SOIL THICKNESS AND MECHANICAL TRANSPORT RATES

Soil thickness is thought to have some influence on mechanical transport rates (Ahnert 1964), and a simple model for the relationship is to assume truncation of the shear rate profile at the "base" of the soil. Thus for an exponential shear profile truncated at depth y_1 :

$$dv/dy = -v_0 \exp(-y/y_0)/y_0,$$

$$v(y) = v_0 \left[\exp(-y/y_0) - \exp(-y_1/y_0) \right]$$

$$S = \int_0^{y_1} v(y) dy = v_0 y_0 \left[1 - (1 + y_1/y_0) \exp(-y_1/y_0) \right]$$

This tends to an upper limit, $v_0 y_0$, at large y_1/y_0 , and behaves like $y_0 y_0 - (y_1/x_0)^2/2$ for small y_1/y_0 . Other plausible velocity profiles give comparable analyses (Figure 4), suggesting that the ratio of actual to maximum transport rate should be treated as an increasing function of the ratio y_1/y_0 , where y_1 is the soil depth and y is a depth characteristic of the alternation of velocity with depth for the slope process.

In the present context, it seems appropriate to use soil deficit in place of soil depth even though the notion of truncation is less well-defined. Thus the potential transport rate has been reduced by a factor, for which one simple form is:

$$\phi(w) = \frac{w^2}{w^2 + 2w_0^2} \quad (8)$$

where w_0 is a soil deficit given by the depth of influence of each slope process. It is expected to take values of 100-500 mm for soil creep or solifluction. For surface wash, soil thickness influences transport rates via grain-size. Although the process operates within the surface 10-20 mm, thin soils tend to be coarse-grained, and transport rates are therefore considerably reduced below maximum values. The influence of soil thickness will be seen to be strongest when soils are very thin, but in many cases has little impact.

5. HILLSLOPE HYDROLOGY

For long term soil and slope evolution, a highly simplified

Figure 4. The influence of soil truncation on sediment transport rates for four assumed velocity distributions with depth.

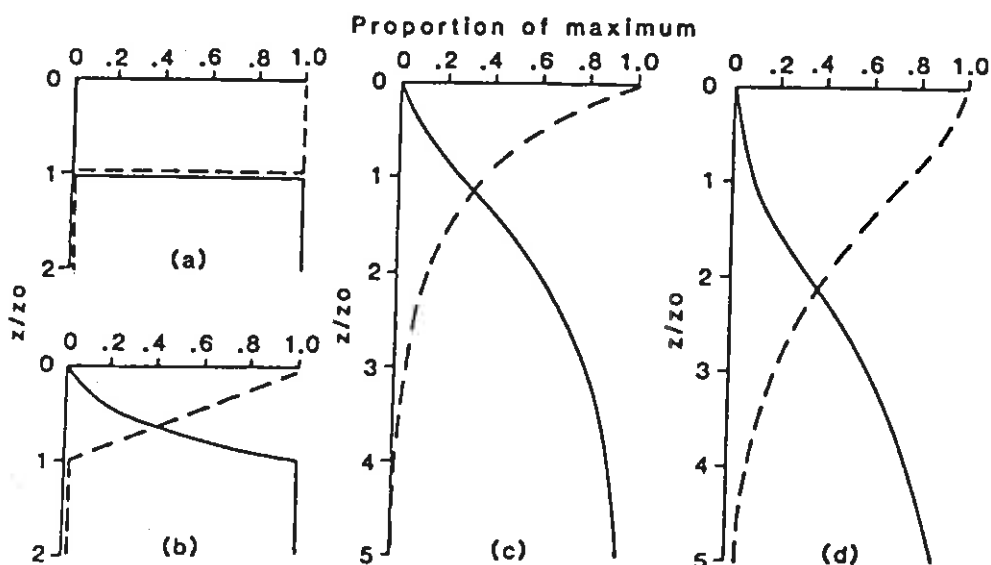
(a) Constant: $\begin{cases} v = v_0 & \text{for } z \leq z_0 \\ v = 0 & \text{for } z > z_0 \end{cases}$

(b) Constant shear: $\begin{cases} v = v_0 (1 - z/z_0) & \text{for } z \leq z_0 \\ v = 0 & \text{for } z > z_0 \end{cases}$

(c) Exponential: $v = v_0 \exp(-z/z_0)$

(d) Modified exponential: $v = v_0 (1 + z/z_0) \exp(-z/z_0)$

Broken curves show velocity distributions. Solid curves show sediment transport for truncation at depth z .



hydrological basis is needed. In this case it is proposed to assume a constant vegetation cover and climate. The vegetation cover and the organic soil derived from it are considered to establish a critical storage capacity, h above which daily rainfall amounts produce overland flow. Annual overland flow produced in this way, summed over the daily rainfall distribution, totals:

$$H_o = P \exp(-h/r_o) \quad (9)$$

where P = annual precipitation

r_o = mean rain per rain-day.

The remaining rainfall is considered to percolate into the soil and be available for evapotranspiration, up to a climatically determined maximum, E_o . An estimate of actual evapotranspiration is then made as:

$$E_A/E_p = (x^n - x)/(x^n - 1) \quad (10)$$

where $x = (P - H_o)/E_p$

n is a constant ≈ 4 .

This expression (figure 5) follows Langbein's (1949) generalized rainfall-runoff curves for U.S.A. The remaining rainfall is next considered to be available for percolation to groundwater, at a rate Q which is characteristic of the bedrock. Any surplus remaining is then available for sub-surface flow:

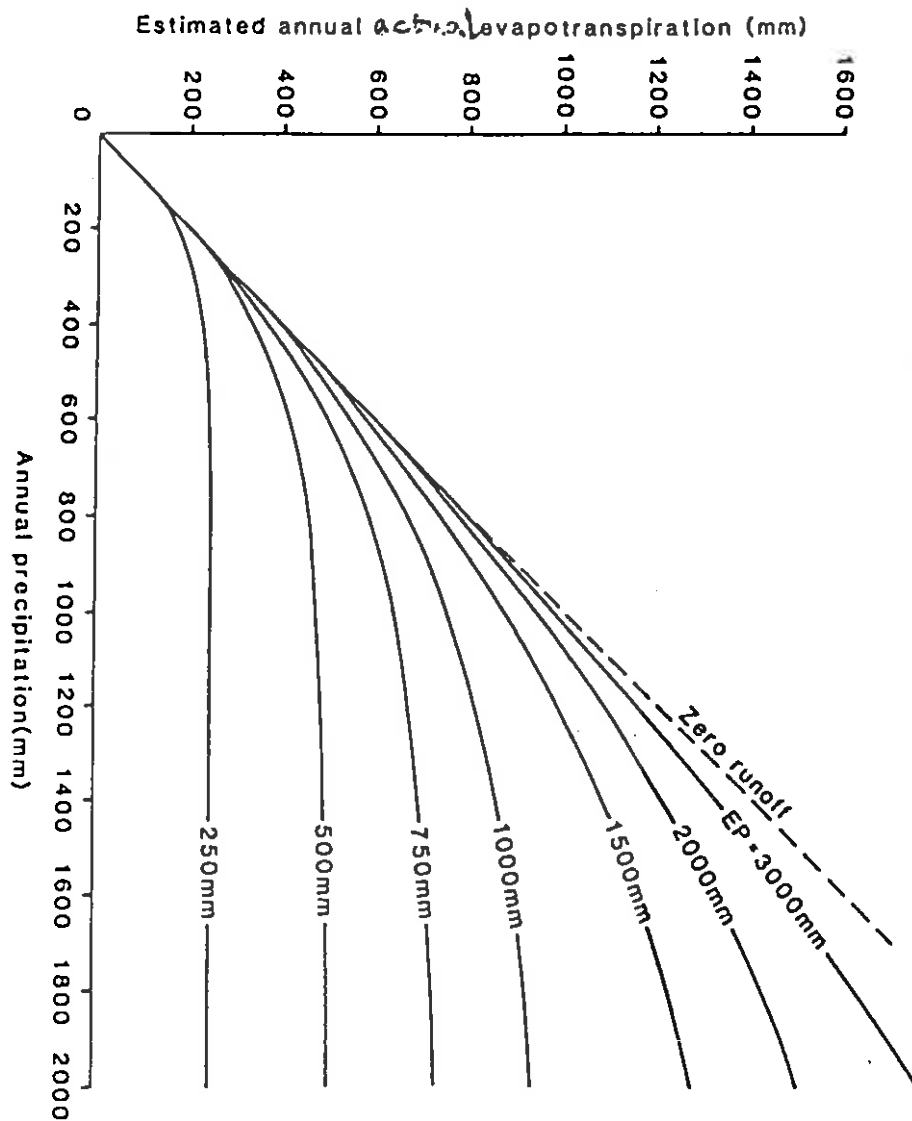
$$-J_o = P - H_o - E_A - Q \quad (11)$$

Subsurface flow is limited by the capacity of the weathered soil to carry it, which may be considered to depend on the soil deficit. For simplicity the total subsurface flow capacity has been taken in the form:

$$q_{\text{max}} = K i \quad (12)$$

where K is an appropriate hydraulic conductivity and i is the local surface gradient.

Figure 5. Generalized estimates for actual evapotranspiration derived using Equation 10. Overland flow has not been subtracted from precipitation to obtain these curves.



Where $\frac{dq_{max}}{dx} < J_0$

then not all the available flow can be carried within the soil, and the excess is added to the accumulated overland flow. The procedure described above establishes the partition between overland flow, which is considered capable of producing wash erosion but too rapid to pick up solutes; and subsurface flow and percolation to groundwater, both of which are considered to pick up solutes at concentrations related to lithology. The impact of these hydrological influences is usually most important for thin soils; although a second important effect is seen for areas of very low gradient, where even deep soils can carry little flow and therefore only small solute loads.

6. SOIL DEPTH AND WEATHERING RATES

It has been widely considered, by Gilbert (1877), Ahnert (1964) and others that the influence of soil depth on weathering rates can best be expressed by a curve in which the rate first increases and then decreases with depth. In the present discussion, the increase is strongly represented through the role of shallow soils in reducing sub-surface flow and hence solute transport. The subsequent reduction in weathering rates for deep soils has not been explicitly modelled, but is to some extent implicit.

The reduction in weathering for deep soils is thought to be due to the very slow circulation of waters through them; so that although solute concentrations are high, removal rates are low. It is argued

here that deep soils generally require very gentle gradients, so that the hydrological effects described above are sufficient to reproduce the expected gradual decline in weathering rates where soils are deep, so that an explicit formulation is not appropriate. At a single site, the proposed hydrological model provides for a linear increase of solutional loss with soil deficit until the soil is thick enough to carry the available component of rainfall, J_0 . For thicker soils, solution then remains constant at $U = cJ_0$.

7. MECHANICAL TRANSPORT PROCESSES

Following most previous work, soil creep and solifluction are considered here to transport material at a rate proportional to tangent slope gradient. Appropriate constants are thought to be 0.001 for soil creep and about 0.01 for solifluction (Carson & Kirkby 1973, Finlayson 1976). The rates obtained are then corrected for soil thickness as described above.

Wash processes have been modelled in a wider variety of ways, although transport rates are most commonly forecast by an expression of the form:

$$S \propto q^m i^n$$

where q = overland flow discharge

and m, n are constant exponents, usually in the range 1-2.5. In many cases distance from the divide is used in place of discharge on the assumption of uniform overland flow production. Here the form adopted is a convenient one within the range indicated, namely:

$$= 0.02q^2 i \quad (13)$$

The constant has been obtained by calibration from erosion data for substantially unvegetated surfaces (Carson & Kirkby, p.216) and assumes that q and S are measured in cubic meters per unit width per year. A lower value for the constant is appropriate for vegetated surfaces due to the substantial flow resistance of plant stems. In the absence of a satisfactory model for variation with soil depth, the correction used has provisionally been taken to be the same as for soil creep and solifluction.

Landslides have been modelled in a rather different way, which is discussed at greater length elsewhere (Kirkby, in prep.), and is only briefly summarized here. As a largely "weathering-limited" process, it seems best to specify denudation rates initially, in terms of lateral slope retreat at gradients above an ultimate threshold. Thus:

$$\begin{aligned} \underline{D} &= 0 & \text{for } i &\leq i_* \\ \underline{D} &= R(i-i_*) & \text{for } i &\geq i_* \end{aligned} \quad (14)$$

where D is the rate of lateral retreat

i_* is the ultimate threshold gradient

and R is a rate constant.

In modelling the evolution of coastal cliffs, a single threshold appeared fully adequate and therefore preferable to the use of a series of thresholds. Values obtained from this study on Old Red Sandstone sequences in South Wales, and by reworking Hutchinson's (1967) historical data on London Clay Cliffs gives some appropriate values for the constants.

	$R(m/y)$	i_*
ORS sandstone/shale sequence	0.001	0.40
London Clay	2.5	0.1

Denudation rates measured vertically may be obtained from D by multiplying by slope gradient.

Because deposition may occur at gradients above the threshold, i_0 ; and because landslides have appreciable travel distances relative to total slope length, a simple weathering-limited model is not sufficient. Instead an erosion-limited model is proposed (Kirkby 1971, Bennett 1974, Foster & Meyer 1975). Denudation is considered to take place at a rate proportional to the difference between transporting capacity and actual transport rate. The link from the free denudation rate, D , to transport capacity is via the travel distance, h ; capacity being equal to their product.

The local vertical denudation rate is then:

$$-dz/dt = Di - S/h \quad (15)$$

In this expression travel distance is also thought to increase with gradient, becoming infinite for talus slopes. The form proposed is:

$$\begin{aligned} h &= h_0/(i_0 - i) \quad \text{for } i < i_0 \\ 1/h &= 0 \quad \text{for } i \geq i_0 \end{aligned} \quad (16)$$

for constants h_0 , i_0 with i_0 usually greater than i_c . For 35° talus slope, $i_0 \approx 0.7$. The use of a constant h_0 is equivalent to an assumption that material is dropped freely from a height h_0 , that its total impact momentum is transferred downslope without loss and that it then comes to rest by sliding on a surface whose angle of friction is $\tan^{-1}(i_0)$. Travel distances should, of course, reflect the difference between maximum and residual angles of internal friction and the effect of cohesion in producing macroscopic slides. The derivation above does not represent the processes acting, but nevertheless indicates the magnitude of the potential energy available in a

landslide. Realistic values for h_0 are thought to lie in the range 5-30 meters.

Between the two critical gradients, i_n and i_0 , the slide process, as modelled, has a meaningful transporting capacity, equal to Dh , which has been compared with rates for creep/solifluction in Figure 6. It may be seen that there is only a narrow range of gradients within which the two sets of processes are comparable in magnitude (a wider range may be applicable where wash is significant). Outside this range, one or other process is overwhelmingly dominant.

8. SLOPE PROFILES AND SOILS UNDER LANDSLIDING

The influence of Equations (14) to (16) may be seen most simply by assuming a constant rate of lateral slope retreat G (which may be + or -). Then from Equation 15:

$$S = hi(D - G) = G(z_0 - z)$$

for some constant x_v .

Substitution in Equations 14 and 16 then given:

$$(a) \quad 0 < i < i_n < i_0 : i = i_0 \frac{(z_0 - z)}{(z_0 - z) - h_0} \quad (17)$$

This gives meaningful values for

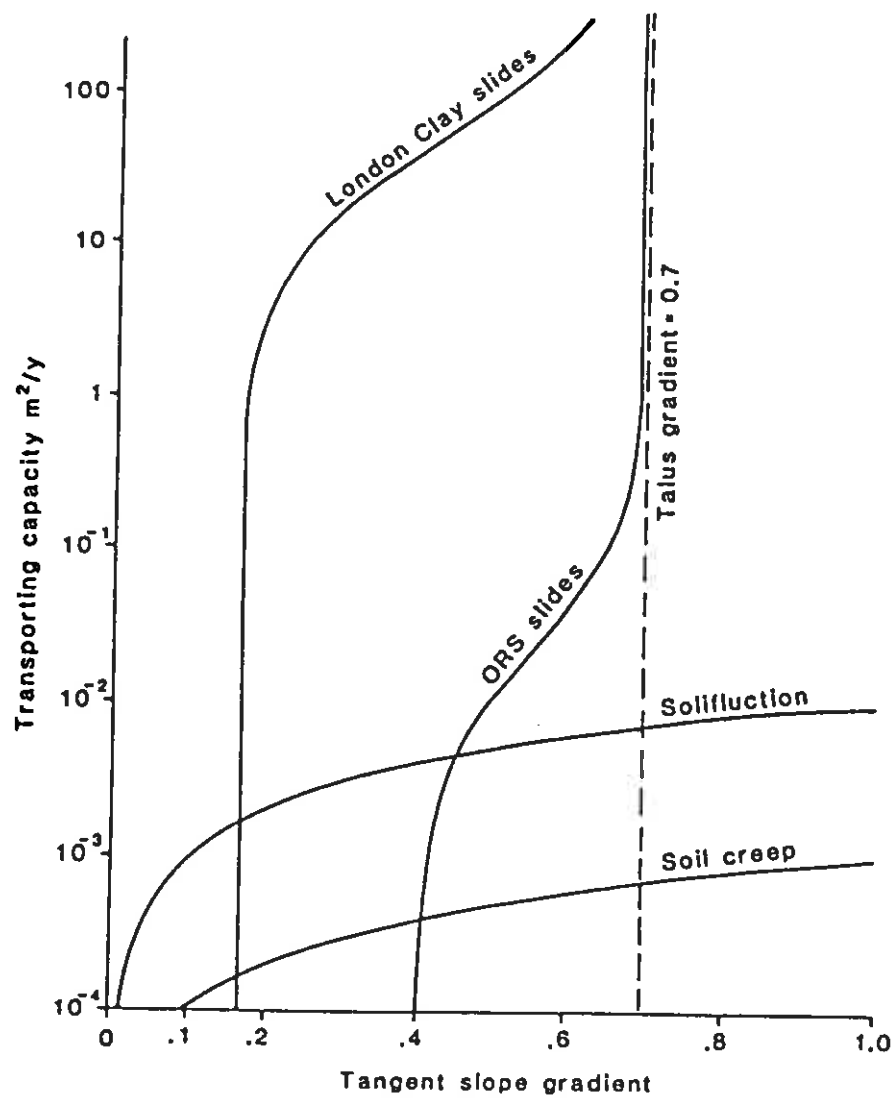
$$0 > (z_0 - z) > -i_n h_0 / (i_0 - i_n) ,$$

which corresponds the concave toe of a talus slope, with z_p at the slope base.

$$(b) \quad -i_n < i < i_0 : Rh_0 i^2 - i [Rh_0 i_n + G h_0 - G(z_0 - z)] - G(z_0 - z) \quad (18)$$

This gives two solutions, only one of them valid.

Figure 6: Transporting capacity for creep, solifluction and, where defined, for landsliding for London Clay and Old Red Sandstone parent materials. Values used as in text.



For slope retreat ($G > 0$) a convex slope is formed, which steepens towards a uniform talus angle downwards. For accumulation slope ($G < 0$), a concave slope develops, straightening upwards towards a talus angle.

$$(c) \quad i_0 < i : i = i_0 + G/R \quad (19)$$

which is a straight slope at an angle which steepens with the rate of retreat. This solution is illustrated in Figure 7.

Figure 8 shows a slightly different solution, in which the rate of retreat is constant over time, but decreases from a positive maximum at the crest to an equal but negative minimum at the base. The slopes derived thus show a simplified version of slopes undergoing free degradation by landslides. For rapid rates of retreat a cliff is formed with accumulation on a slope close to the talus gradient. At low rates of retreat, profiles are smoothly concave throughout. In all cases, a run-out concavity forms at the slope base at gradients below the threshold angle. The scale of the entire slope is largely determined by choice of the travel distance parameter, k_0 . The long-term evolution of an initial cliff may be approximated by arranging these profiles in sequence. Even though the assumptions of constant retreat over time and a change from erosion to deposition at mid height are thereby violated, the more exact numerical solution closely parallels this sequence (with profiles crossing at mid height).

It may be seen, from the formulation of Equations 14 to 16 above and from Figure 1, that soil thickness and/or weathering is not treated as an influence on the rate of sliding, but only as a result of sliding. The argument for making this assumption is that soils are thin, and not necessarily derived from the bedrock on which they are lying (increasingly downslope), so that the crucial geotechnical

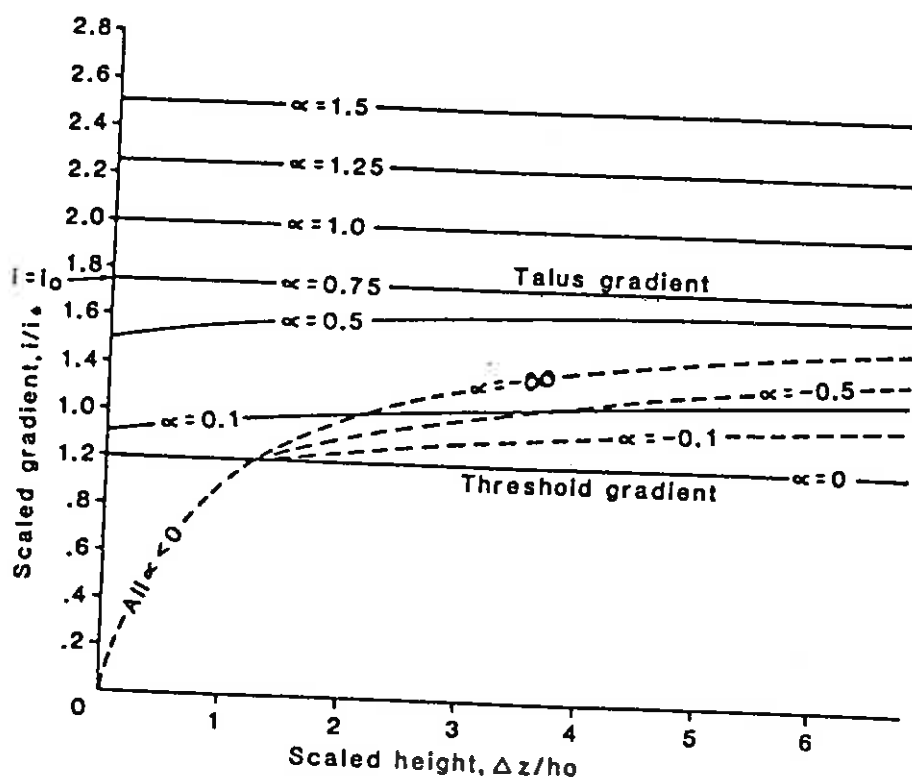


Figure 7. Equilibrium gradients for constant rates of retreat ($\alpha \geq 0$: solid curves) or accumulation ($\alpha < 0$: broken curves). Height difference Δz measured below crest of retreating slopes and above base of accumulation slopes.

$\alpha = G/(R_{\text{max}})$ where G is rate of lateral retreat.

Other notation as in Equations 14 and 16.

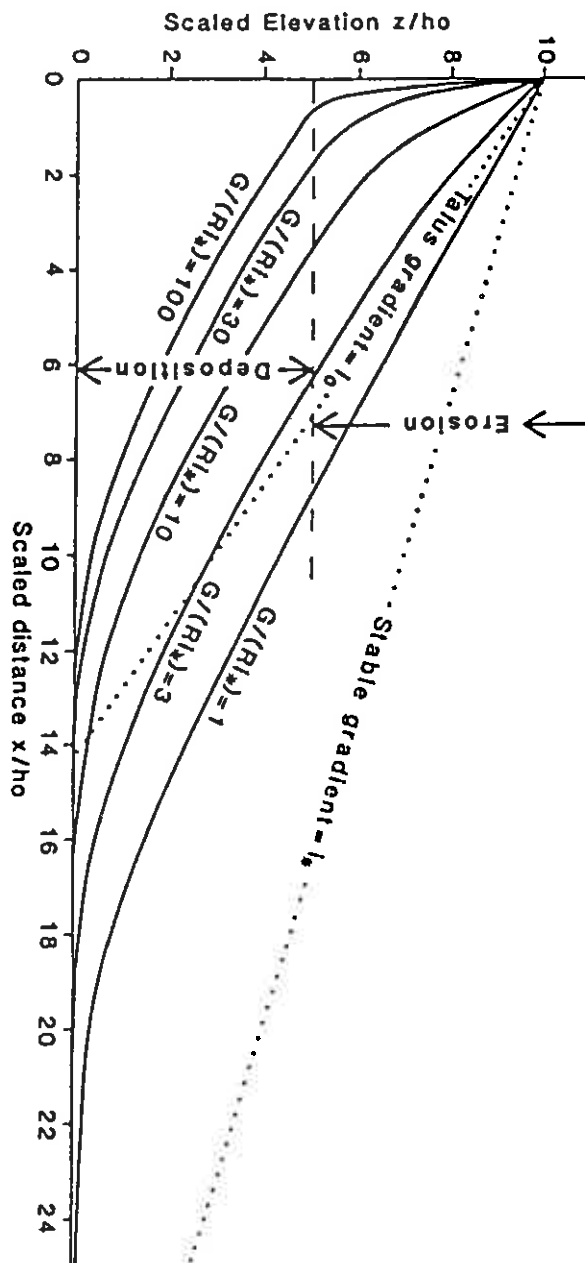


Figure 8. Model slope profiles in equilibrium with landsliding, where retreat is at rate G at top of slope, and decreases linearly to $-G$ at base. Curves correspond to retreat for slopes of various gradients. Dotted lines show assumed talus (i_0) and stable (i_s) gradients.

variables relate to the weathering front zone and so primarily to the bedrock rather than to the soil properties. Nevertheless, if the vertical denudation rate is assumed constant over time, and the solutional denudation loss, U is taken as fixed, then there is a clear relationship between equilibrium soil thickness, indicated by:

$$\pi_s = (i - p_s) / p_s,$$

and the slope gradient. This relationship is shown in Figure 9, and is given by:

$$\left. \begin{aligned} & \pi_s R L_*^2 / U = 1/B \\ & i_0 \leq i : i/i_* = [1 + \sqrt{(1+B)}] / 2 \\ & i_* < i \leq i_0 : i/i_* = \alpha + \sqrt{\alpha^2 + (i_* x h_0 + 1)B} \end{aligned} \right\} \quad (20)$$

where $\alpha = (1 - i_* x B / h_0) / 2$

For thin soils and gradients at least as steep as talus, the relationship is single-valued, but shows a dependence on position, x for lower gradients, due to the influence of material deposited from upslope. In most cases this influence is rather slight, as is indicated by the curves shown. For the parameter values used, the curve for $x' = 1.5$ corresponds to a slope length of 100 m.

9. SLOPE PROFILES AND SOILS UNDER CREEP/SOLIFLUCTION AND WASH

As with landslides, the interaction of slopes and soils can be seen most simply by assuming uniform rates of change. For the transport limited processes, it will be assumed that rates of total vertical denudation are constant over time; and constant or changing in a prescribed fashion downslope. Local rates of solutional denudation

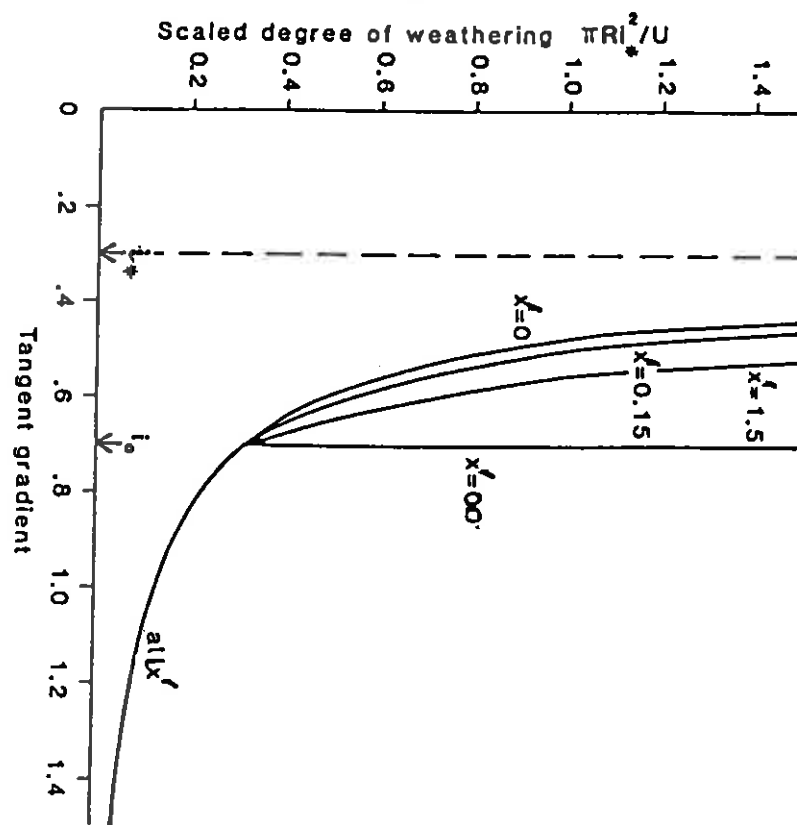


Figure 9. The modelled relationship between slope gradient under landsliding and degree of soil weathering, assuming constant downcutting rates and constant solution loss U . Scaled distance from divide, $x' = i_* x / h_0$

are also assumed constant over time, and varying downslope, corresponding to vertical rock stratification. For simplicity it will be assumed that the soil can everywhere carry sufficient sub-surface flow and/or percolation to give maximum rates of solution; and overland flow increasing linearly downslope.

At a distance x from the divide:

$$S = (\bar{Y} - \bar{u})_x = \beta_s [\phi + (x/x_0)^2] \quad (21)$$

where \bar{Y} is the average rate of total denudation from the divide.

u is " " " " solutional denudation " " "

β is the rate constant for soil creep/solifluction,

S is slope gradient at x .

ϕ is the correction factor for creep/solifluction in thin soils (cf Equation 8),

and x_1 is the distance from the divide at which wash rates become equal to those for creep/solifluction (cf Equation 13).

Slope gradient is then given by:

$$\beta s = (\bar{y} - \bar{u})x / [\phi + (x/x_c)^2] \quad (22)$$

Differentiating with respect to distance:

$$\frac{x}{s} \frac{ds}{dx} = \frac{x_i^2 - x^2}{x_i^2 + x^2} - \frac{\bar{\gamma} - \gamma}{\gamma - \bar{u}} - \frac{x^2 d\phi/dx}{x_i^2 + x^2} + \frac{\bar{u} - u}{\gamma - \bar{u}} \quad (23)$$

where \bar{Y} , \bar{U} are the local rates of total and solutional denudation respectively [i.e. $\bar{Y} = d/dx(\bar{Y}x)$].

The four terms on the right hand side of Equation 23 may be described as follows:

- (a) the first term shows the normal change in response to the downslope action of slope processes. For creep/solifluction alone, $x_1 \rightarrow \infty$ and this term takes the value 1.0, representing a constant convexity. Otherwise, gradient increases for $x < x_1$, and decreases for $x > x_1$, giving a convexo-concave profile. The magnitude of this first term expresses the "standard" response of the slope for a uniform lithology and constant downcutting, and subsequent terms are superimposed upon it.
- (b) the second term (mainly) shows the influence of variations in total denudation rate. For example if, as is normal for mature slopes the local rate and average decline downslope, then this term is negative, indicating less convexity or greater concavity than under conditions of constant downcutting. The magnitude of this term commonly increases downslope, corresponding to a monotonic reduction in local downcutting rates.
- (c) the third term shows that wherever soils thin ($d\phi/dx < 0$) downslope, slopes will relatively steepen. This effect is strongest over the range of soil deficits where $\phi(w)$ responds most strongly: that is $w < 5w_0$, and especially near $w = w_0$.
- (d) the final term shows the effect of lithological differences acting via solution rate. Where the local parent material is less soluble than the average from the divide (i.e. $\bar{U} > U$), slopes will steepen relatively; and where the local rock is more soluble than average, slopes will become relatively gentler. Thus if the standard response to process were a straight slope, hard rock bands would produce convexities and soft rock concavities in the profile.
- In summary therefore, the analysis of Equations 22 and 23 shows that the effect of lithology is to produce relative steepening

of the profile where the underlying rock is less soluble than average and/or where soils thin downslope. It will be seen that these effects commonly reinforce one another. However because differences in soil thickness have most influence at sites where the soil is generally thin, such sites show the greatest response of slope gradient to lithology.

The response of the soil to changes in lithology can be indicated roughly by assuming that soil has reached equilibrium. Even though time spans are commonly insufficient to justify this assumption, it is able to show the direction of expected differences, while over-estimating the magnitudes likely to be observed in practice. Figure 10 illustrates the kind of forms to be expected, assuming that soils have reached equilibrium with the constant downcutting rate, and that the gradients obtained are less than landslide thresholds for the materials in question. In the example solifluction/creep is considered as the only mechanical process, so that where the "resistant" bands are the same as the remainder of the rock ($u^f/u = 1.0$), the soil is of constant depth and slope gradient increases linearly downslope. As the resistant bands are considered to be progressively less soluble, each band shows an exaggeration of the convexity with soil thinning downslope over the hard band, followed by a less marked concavity with thickening soils as gradient and soil recover towards their previous values.

Where soils become thin locally, diversion of sub-surface flow overland will tend to reduce local solutional denudation, and still further accentuate the response to lithological differences indicated by Equation 23 above. However this diversion will also increase overland flow, and the slopes will tend to respond by evolving

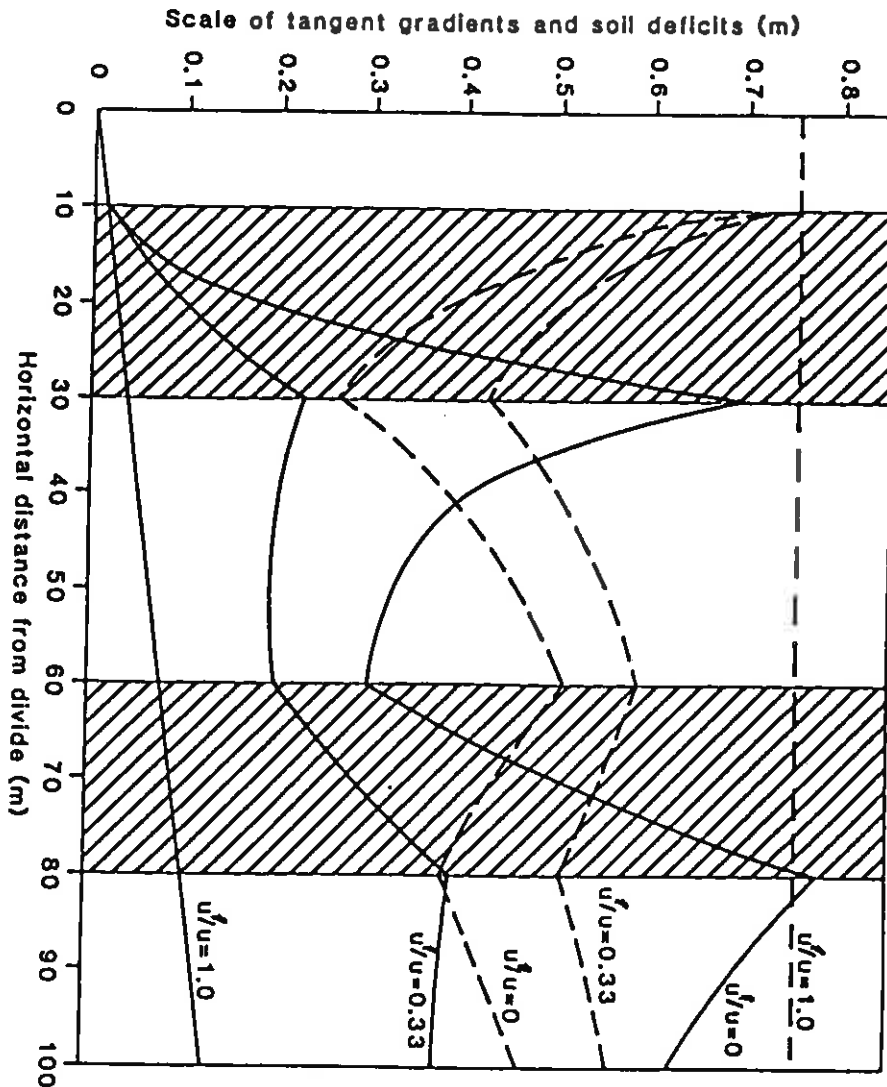


Figure 10. Modelled response of gradient (solid curves) and equilibrium soil deficit (broken curves) on a hillside undergoing constant total denudation at $20 \mu\text{m}/\text{year}$. Rock solution in unshaded zones at $U = 15 \mu\text{m}/\text{year}$, and in shaded zones at $U' = 0-15 \mu\text{m}/\text{year}$. Note the convexity of the less soluble bands, and the weakening response downslope.

towards lower gradients. The combined influence of the flow diversion is therefore not immediately apparent.

10. AN INTEGRATED SLOPE EVOLUTION MODEL

The various processes described above have all been combined in a digital computer program to simulate some examples of slope profile, and soil evolution. The model solves the partial differential Equations 1 and 3 using an explicit method, and selects the iteration time-step so that gradient and soil thickness change by less than a specified proportion at all points.

The boundary conditions at $x = 0$ is specified as a divide so that $S = 0$ and $V = 0$ at this point. At the basal point, the boundary condition is specified by expressions for elevation and soil thickness at a fixed value of x . In the examples used here, elevation has been held constant at the basal point, an assumption which normally leads to Davisian decline or "characteristic form" solutions in simple cases. A corresponding condition for soil is less obvious. Fixed basal elevation is usually supposed to correspond to a basal river removing all debris supplied to it at a base-level which is fixed in height. Under such circumstances it is artificial to set soil thickness to a fixed value, since weathering may proceed beneath the river bed. Nor are symmetry conditions of zero transport, like those used for the divide, appropriate at a basal river, although they would be appropriate for the base of an infilling, undrained valley. The condition adopted has been for symmetry with non-zero transport,

that is for

$$dw/dx = 0$$

at the slope base. This condition implies negligible interference by the basal river on the base of the soil profile, and appears to be at least a neutral choice, appropriate in the absence of other constraints.

Lithology has been represented as a sequence of parallel strata at any specified inclination. Each stratum is assigned a thickness, and process parameters for solute concentration (c in Equation 4), landslide threshold and rate of sliding above it (i_* and R respectively in Equation 14). All other parameters have been given the same values for all strata. Example runs have been carried out for slopes divided into 40 horizontal increments. This resolution limits the number of distinct strata which can usefully be included to three or four.

All of the linkages shown in Figure 1, and discussed above, have been incorporated into the model. Climate is explicitly represented by a set of hydrological parameters which define the initial partition of flow, but it is recognised that climate will also have some influence on a number of process parameters. Perhaps the most important such implicit effects are on the solute concentration (via vegetation and soil CO_2 levels); on the landslide rate parameter, R (via solute rates); and on the creep/solifluction rate parameter (via freeze-thaw frequency and vegetation cover). Similarly lithology implicitly influences all soil parameters, which may consequently vary downslope, and through them most process parameters.

Figures 11 and 12 show illustrative runs of the model. The table below lists the parameter values used in these runs. The values used

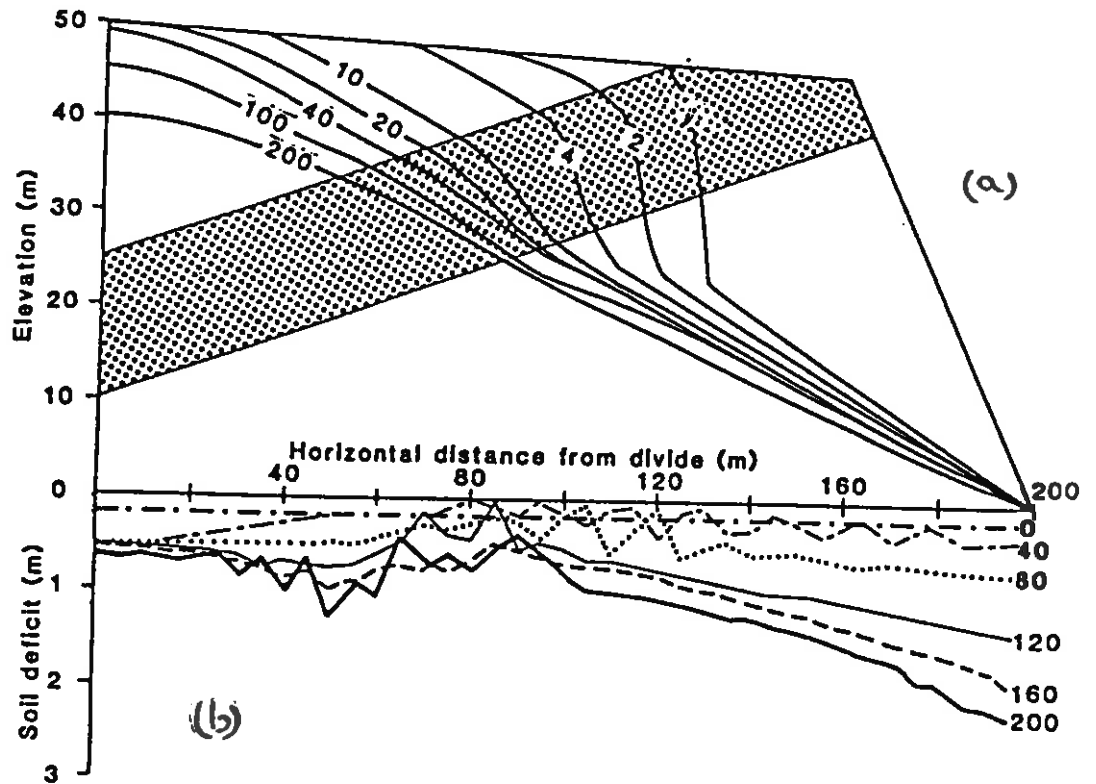


Figure 11. Simulation of slope development for initial form shown, with a hard band dipping at 10° into slope.

	Properties of strata are:		
	C	R	λ
Shaded (hard) band	1×10^{-6}	0.005 m/y	0.25
Unshaded (soft) bands	50×10^{-6}	0.5 m/y	0.25

(a) Slope profile evolution.

(b) Soil deficit evolution.

lie within the ranges proposed above on the basis of knowledge of individual processes, but would need some optimization before detailed field comparisons could be made.

Parameter values used in illustrative numerical simulations

<u>Parameter</u>	<u>Value & Units</u>	<u>Equation</u>
Creep solifluction rate	$0.01 \text{ m}^2/\text{y}$	-
Wash rate	$0.02 \text{ y}/\text{m}^2$	13
Landslide travel distance	$h_0 = 20 \text{ m}$	16
Talus gradient	$i_0 = 0.7$	16
Groundwater percolation	$Q = 150 \text{ mm}/\text{y}$	11
Soil permeability parameter	$K = 5000 \text{ m}^2/\text{y}$	12
Limiting degree of weathering	$\pi_F = 1.5 \text{ } (\rho_F = 0.4)$	5
Rate of change of soil deficit with weathering	$w_1 = 2 \text{ m}$	5
Scale depth to allow full transport	$w_0 = 0.5 \text{ m}$	8
Annual rainfall	$P = 1000 \text{ mm}/\text{y}$	9, 11
Number of rain-days	$P/r_0 = 175/\text{y}$	9
Potential evapo-transpiration	$R_p = 500 \text{ mm}/\text{y}$	10
Soil "A" horizon storage for daily rainfall	$h = 80 \text{ mm}/\text{day}$	9

The initial slope form chosen has either been a gently sloping plateau terminating in a steep bluff (Figure 11) or a uniform gradient at the landslide-stable gradient i_0 (Figure 12). In all cases an initial uniform soil deficit of 0.1 to 0.5 m has been assumed. A single more resistant layer has been included in the slope strata,

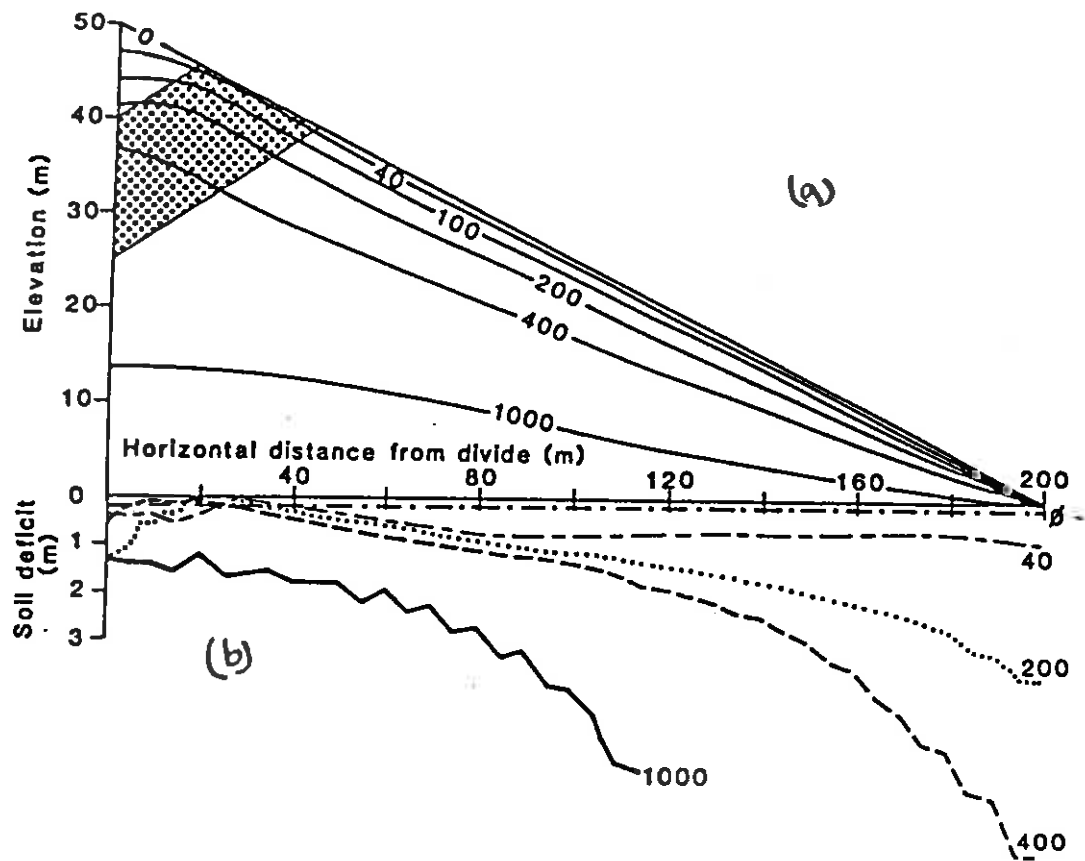


Figure 12. Simulation of slope development with hard band dipping at 20° .

Properties of the strata are:

	C	R	f_1
Shaded (hard) band	1×10^{-6}	.01 m/y	.25
Unshaded (soft) bands	50×10^{-6}	.01 m/y	.25

(a) Slope profile evolution.

(b) Soil deficit evolution.

dipping at 10° to 20° into the slope. Each figure shows the evolution of the overall slope topography (a) and of soil deficits (b).

Figure 11 shows a hard band which is less soluble and has a lower rate of landslide retreat (R) than the softer strata on either side, but the same ultimate threshold gradient for landsliding ($i_{*} = 0.25$). Slope development (Figure 11a) shows rapid development of gradients close to the threshold for the softer strata, with undercutting of the harder rock, which initially steepens considerably and then very gradually declines, so that after 200 000 years it has little topographic expression. The steep section comes to coincide with the hard strata after a few hundred years (within the resolution of the model). After approximately 20 000 years, a summit convexity begins to replace the threshold slope above the hard band, and this process is substantially complete after 200 000 years. At the end of this period, however, the lower slope although no longer subject to sliding, still stands at an almost constant gradient (0.22) just below the landslide threshold. Under the assumed climate little wash is evident. Soils initially thicken due to weathering on the plateau, and are stripped by landslides below. As slides occur locally, the soil distribution is very uneven. The size of slides shown is an artefact of the computational time-step rather than a true representation of individual events, but nevertheless appears to mimic reality. Once slopes begin to stabilize, soil is again able to thicken everywhere. It shows the expected increase downslope and over time, but with a decrease within the less soluble hard band, which is in the direction indicated in Figure 10, and becomes more marked over time.

Figure 12 shows the effect of solubility differences alone, with an initial form at the limit of landslide stability. The overall slope

evolution consists of the development of a convexo-concave slope on which wash eventually predominates over the lower half of the slope, and soils thicken progressively downslope. Within the insoluble band, however there is local steepening so that landsliding occurs there to a small extent. Beneath the insoluble band, a compensating concavity develops before the slope reverts to its "normal" trend of convexity in the upper half of the profile. Soils thin downslope over the insoluble band, and thicken elsewhere, with the trend to thickening developing from the divide downwards. The simulation thus shows the effect of a less soluble band which is illustrated in Figure 10. It also shows the tendency to approach soil equilibrium soonest where downcutting is most rapid (near the divide in this case).

11. CONCLUSIONS

A number of provisional deductions may be made from the model simulations, and from the analyses of individual processes in sections 8 and 9 above. These deductions appear to correspond to features of real landscapes, and so encourage detailed comparisons between model and field data, after due allowance has been made for evidence of slope-base and climatic history.

Geotechnical properties, especially the rate of decline towards the threshold (R), influence landforms much more strongly than solutational properties. The latter only begin to play a dominant role on slopes of low gradient and after long times. In common stratigraphic associations, like limestone/shale or sandstone/shale sequences, the rock which is considered to be "more resistant" appears to be

geotechnically stronger but more soluble than the "less resistant" shales. Gradients close to landslide thresholds commonly outlive landslide activity for many thousands of years, and so play perhaps the dominant role in determining regional relief in a tectonically stable area.

Soils are generally thin under active landsliding and wash. Thick soils thus tend to indicate the predominance of solution and creep/solifluction in landscape denudation. In a humid climate, and where downcutting is least near the slope base and greatest near divides, it is to be expected that soils will eventually thicken downslope. They commonly approach a quasi-equilibrium with current rates of denudation, and approach it sooner at upslope than downslope sites. In this way pronounced soil catenas are developed due to the balance between mechanical processes and solution. Over time, as elevations decline, mechanical denudation falls steadily while solution remains relatively constant, so that the quasi-equilibrium is steadily shifting towards deeper soils over time. Under semi-arid conditions the greater importance of wash produces thin soils except on very low gradients. The catenas developed are likely to be reversed, with deeper soils upslope and shallower soils downslope.

There is no evidence for any significant hangover from previous positions, as erosion changes outcrop location on the slope (except for vertical strata). Within the resolution of the model, gradient steepening and soil thinning downslope over resistant strata is thus strictly associated with the current outcrop location. Small proportions of resistant strata appear to have a disproportionate effect in steepening the slope profile overall. The resistant bands, by maintaining locally steep gradients, tend to hold the less resistant

strata close to their threshold gradients, and so increase gradients everywhere.

In conditions where wash is important, then simulated slope retreat commonly consists of a steep slope at a gradient determined by sliding, with basal replacement (dominated by wash) from an early stage producing a pediment-like feature which is progressively regraded, and has little soil developed on it as long as its evolution remains active (i.e. until incision for example).

Under generally thin soils associated with rapid sliding or wash, the model shows periods during which soil thickness fluctuates appreciably downslope, and travels as a wave over time. Although it is recognised that the scale of these effects ^(in the model) results from the dynamic choice of the simulation time step, the sediment waves are thought to provide a helpful analogue of episodic landsliding and discontinuous soil erosion. In the case of landslides, soil accumulation builds up local gradients to trigger slides downslope in a cyclic fashion. For wash, thin soil areas produce larger volumes of overland flow, and so localize erosion and produce local deposition downslope. Denudation reduces the local gradient until it is too low to produce erosion and its locus then tends to shift upslope.

The model is thought to reflect reality in that slope and soil evolution is highly sensitive to the exact criteria for overland flow and wash transport. Particular care would be needed in optimising relevant parameters before making particular field comparisons. Such comparisons have not been attempted here, but clearly represent the next stage in validating this model.

REFERENCES CITED

- Ahnert, F. 1964. Quantitative models of slope development as a function of waste cover thickness. Abstr. of Pap. 20th I.G.U. Congress, London, 198.
- Ahnert, F. 1967. The role of the equilibrium concept in the interpretation of landforms of fluvial erosion and deposition. I.G.U. Slopes Commission Report 6, 71-84.
- Ahnert, F. 1970. Functional relationships between denudation, relief and uplift in large, mid-latitude drainage basins. Am. J. Sci. 268(3), 132-63.
- Bennett, J.P. 1974. Concepts of mathematical modelling of sediment yield. Water Resources Research 10(3), 485-92.
- Carson, M.A. and Kirkby, M.J. 1973. Hillslope form and process, Cambridge.
- Culling, W.E.H. 1963. Soil creep and the development of hillside slopes. J. Geol. 71, 127-62.
- Finlayson, B.L. 1976. Measurements of geomorphic processes in a small drainage basin. Unpub. PhD Thesis, University of Bristol.
- Foster, G.R. and Meyer, L.D. 1975. Mathematical simulation of upland erosion by fundamental erosion mechanics, in Present and prospective technology for predicting sediment yields and sources. Proc. Sediment Yield Workshop, USDA Sedimentation Lab., Oxford, Miss. Ag. Res. Service Report ARS-S-40, 190-207.
- Gilbert, G.K. 1877. Report on the geology of the Henry Mountains. US Geol. Survey, Washington.

- Huggett, R.J. 1975. Soil landscape systems: a model of soil genesis. Geoderma 13, 1-22.
- Hutchinson, J.N. 1967. The free degradation of London Clay cliffs. Proc. Geotech. Conf. Oslo 1, 113-18.
- Kirkby, M.J. 1971. Hillslope process response models based on the continuity equation. Inst. Brit. Geogr. Spec. Pub. 3, 15-30.
- Kirkby, M.J. 1976a. Soil development models as a component of slope models. Earth Surf. Proc. 2, 203-230.
- Kirkby, M.J. 1976b. Hydrological slope models - the influence of climate Ch.8 in Geomorphology and Climate ed. E. Derbyshire. John Wiley, Chichester, p.247-67.
- Kirkby, M.J. 1982. The basin for soil profile modelling in a geomorphic context. Leeds Univ. School of Geography, W.P. 301, 20pp.
- Kirkby, M.J. - in preparation. Landslide models in the context of cliff profiles in S. Wales.
- Langbein, W.B. 1949. Annual runoff in the United States. US Geol. Survey Circular 52.